Annals of Biomedical Engineering, Vol. 42, No. 4, April 2014 (© 2013) pp. 843–857
DOI: 10.1007/s10439-013-0962-8

Comparison of Different Material Models to Simulate 3-D Breast Deformations Using Finite Element Analysis

MAXIMILIAN EDER,[1] STEFAN RAITH,[1] JALIL JALALI,[1,2] ALEXANDER VOLF,[1] MARKUS SETTLES,[3] HANS-GÜNTHER MACHENS,[1] and LASZLO KOVACS[1]

[1]Research Group CAPS—Computer Aided Plastic Surgery, Department of Plastic Surgery and Hand Surgery, Klinikum rechts der Isar, Technische Universität München, Ismaninger Str. 22, 81675 Munich, Germany; [2]Institute of Medical Engineering at the Technische Universität München (IMETUM), Boltzmannstr. 11, 85748 Garching, Germany; and [3]Department of Radiology, Klinikum rechts der Isar, Technische Universität München, Ismaninger Str. 22, 81675 Munich, Germany

(*Received 10 August 2013; accepted 7 December 2013; published online 18 December 2013*)

Associate Editor Peter E. McHugh oversaw the review of this article.

Abstract—Biomechanical breast modeling using finite element (FE) analysis to predict 3-D breast deformations is of interest for various biomedical applications. Currently no consensus of reliable magnitudes of mechanical breast tissue properties exists. We therefore applied 12 material properties proposed in the literature to FE simulation models derived from prone MRI breast datasets of 18 female volunteers. A gravity free starting position is computed with an iterative FE algorithm followed by the calculation of the upright position of the breast and then compared to the real breast geometry in standing position using corresponding 3-D surface scans to determine the accuracy of the simulation. Hyper-elastic constitutive models showed superior performance than linear elastic models which cannot exceed the linear Hookean domain. Within the group of applied hyper-elastic material models those proposed by Tanner *et al.* (Med Phys 33:1758–1769, 2006) and Rajagopal *et al.* (Acad Radiol 15:1425–1436, 2008) performed significantly ($p < 0.01$) better than other material models. The advantage of the method presented is its non-invasive character by combining 3-D volume and surface imaging with automated FE analysis. Thus, reliable biomechanical breast models based on the presented methods can be applied in future to derive patient-specific material parameter sets to improve a wide range of healthcare applications.

Keywords—Breast biomechanics, Finite element analysis, Hyper-elastic material model, Numerical simulation, 3-D surface imaging.

Address correspondence to Laszlo Kovacs, Research Group CAPS—Computer Aided Plastic Surgery, Department of Plastic Surgery and Hand Surgery, Klinikum rechts der Isar, Technische Universität München, Ismaninger Str. 22, 81675 Munich, Germany. Electronic mail: l.kovacs@lrz.tum.de

Maximilian Eder and Stefan Raith contributed equally to the article and share first authorship.

INTRODUCTION

Breast cancer is the leading cause of female cancer deaths worldwide with approximately 2.6 million US women alive showing a history of breast cancer and estimated 230,480 new diagnosed female cases of invasive breast cancer in 2011 in the US solely.[1] Breast cancer screening, detection, and diagnosis includes the interpretation of varying clinical images using different imaging modalities such as X-ray mammography, magnetic resonance imaging (MRI), ultrasound, or positron emission tomography (PET). The detection and tracking of tumors or suspicious lesions across different imaging techniques and over different time points need to be highly accurate to ensure the optimal oncologic treatment.[21] The soft tissue of the breast is subject to significant deformations caused by varying external mechanical loads during the different imaging procedures, such as gravity-loading during MRI or biopsies, indentation during ultrasound or compression during X-ray mammography.[22] Therefore, biomechanical breast models employing continuum mechanics have been a subject of interest in the medical and computer science field for simulating mechanical deformations of the female breast of varying medical procedures including non-rigid multimodal image registration,[27] image guided biopsies,[3,4] X-ray mammography compression,[24,29] or breast surgery planning.[5,15,23] A reliable biomechanical breast model could be helpful to predict the movement of suspicious tissue lesions during the imaging procedures and could simplify clinical tumor tracking by integrating comparison of multimodality images into the simulation model.[18,21,29,30] However, a wide range of

values for the constitutive material parameters of the different breast tissue components (see Table 1) has been applied in the past decade[3,5,14,15,21,24–26,30–32] and essential biomechanical requirements must be fulfilled for a realistic breast deformation simulation.[21,22] For example, a realistic mechanical simulation of large breast deformations requires (a) an unloaded reference configuration of the breast geometry as a correct starting loading condition, (b) a geometric model of the anatomical area of interest with (c) valid boundary conditions, and (d) a robust material constitutive model.[5,21,22]

Therefore, the presented work applies an iterative algorithm for the approximation of the stress-free unloaded reference state of the breast for further finite element (FE) simulation. The study aim is to evaluate 12 different parameter sets for material properties (see Table 1) under constant boundary conditions on three-dimensional (3-D) breast models of 18 female test persons derived from MRI in prone position. The accuracy of the FE simulated breast deformation starting from the prone position to the upright position is analyzed by comparing the resulting breast surface displacement to the actual breast geometry of all female volunteers in a standing position using corresponding 3-D surface scans. With this workflow it is possible to evaluate whether a certain material formulation is suitable for the FE simulation of 3-D breast deformations.

MATERIALS AND METHODS

An overview of the developed workflow to simulate and analyse 3-D breast deformations is shown in Fig. 1. The Declaration of Helsinki protocols were followed and all 18 female volunteers included in the study gave their written informed consent in accordance with the approval of the Ethical Committee of the Medical Faculty at the Klinikum rechts der Isar, Technische Universität München, Germany.

The participants mean age was 26.9 ± 3.0 years (range 22–33), with a mean BMI of 21.3 ± 1.7 kg/m^2 (range 18.5–24.2), a mean sternal notch to nipple distance of 19.2 ± 1.7 cm on the right (range 16.5–21.9) and 19.2 ± 1.6 cm on the left side (range 17.0–22.0); a mean breast volume of 382 ± 114 cc on the right (range 176–593) and 371 ± 113 cc on the left side (range 173–584), indicating no existing breast asymmetries. Test persons with a known history of breast cancer or hereditary risk of breast cancer, acute breast infections, known autoimmune or infectious diseases, severe breast malformations and thoracic deformations or fibrocystic mastopathy and previous breast surgeries were excluded from the study.

Image Data Acquisition

3-D Surface Imaging

3-D breast surface imaging was performed using a laser scanner (Konica–Minolta Co., Ltd., Osaka, Japan) applying the principle of triangulation with a mean scanner resolution of 0.4 mm and a mean acquisition time of 2.5 s as reported in preliminary studies.[6,7,11–13,19] 3-D surface scans of all participants were performed in standing position on predefined markers on the ground under standardized lighting conditions (light intensity 350–400 lux) with a 10° upward angle of the scanner facing the participants +30, 0, and −30° relative to the lens.[13] During acquisition the females held their breath with arms down the side at the height of the pelvis and the back was supported by a wall to guarantee reproducible data by minimizing potential artefacts due to movements. The acquired single shots from different angles of each volunteer were converted into virtual 3-D models using appropriate software (Geomagic Studio 12®, Raindrop Geomagic, Inc., NC, USA) without holes or intersections.[6,7,11–13,19]

Magnetic Resonance Imaging

Volumetric MRI data of the 18 volunteer's thorax were acquired by means of Philips Achieva 1.5 Tesla MRI scanner (Philips Medical Systems DMC GmbH, Hamburg, Germany) using a T1-weighted imaging sequence with a 512 × 512 × 179 voxel resolution and a voxel size of 0.994 × 0.994 × 2 mm^3 (imaging parameter: 4.6 ms echo time and 9.2 ms repetition time). Breast images were obtained with the participants lying with arms down the side at the height of the pelvis in gravity-loaded prone position from 3 cm above the clavicle down to the umbilical region without intravenous contrast medium application. In order to avoid any compression of the breast soft tissue, the females were supported by individually modelled foam blocks on the relatively stiff regions of the clavicles and shoulders as well as on the lower belly and bony pelvic region with sufficient distance to the breast to avoid any external breast compression. Thus the shape of the free hanging breast could be acquired in a deformation state only loaded by gravity; a well-defined boundary condition that can be easily applied in the subsequent FE simulations.

Finite Element Simulation

FE Geometry Model Generation

FE models of the breast were generated from the acquired MRI scans of the 18 participants in prone position. The images were saved in DICOM format and loaded into the Mimics® 14.0 software

TABLE 1. Overview of the applied constitutive models that were used as mechanical properties for breast soft tissue in the study.

Lead author	Constitutive model	Experimental condition	Material constants	Material model no. in our study
Krouskop *et al.*[14]	Piecewise-linear elastic	*Ex vivo* indentation test	$E = 18 \pm 7$ kPa at 5% strain $E = 20 \pm 8$ kPa at 20% strain $\nu = 0.495$	Base model for mat6 and mat7
Wellman *et al.*[32]	Piecewise-linear elastic	*Ex vivo* indentation test	$E = 4.8 \pm 2.5$ kPa at 1% strain $E = 17.4 \pm 8.4$ kPa at 15% strain	Base model for mat8 and mat9
	Exponential elastic		$E = b \cdot e^{m\varepsilon} b = 4.46$ kPa & $m = 7.4$	
Azar *et al.*[3]	Exponential elastic	*Ex vivo* based on Wellman *et al.*[32] with a correction for fat	$E = b \cdot e^{m\varepsilon}$ if ε<15.5% $b = 4.46$ kPa $m = 7.4$ if $\varepsilon \geq 15.5\%$ $b = 15.1$ kPa $m = 10$ $\nu = 0.49999$	Base model for mat4 and mat5
Samani *et al.*[24]	Polynomial elastic	*Ex vivo* indentation test	$E = 519.7\varepsilon^2 + 2.4\varepsilon + 4.9$	Based on Wellman *et al.*[32]
Samani *et al.*[25]	Hyper-elastic Mooney-Rivlin with five parameters		$C_{10} = 0.31$ kPa $C_{01} = 0.3$ kPa $C_{20} = 3.8$ kPa $C_{11} = 2.25$ kPa $C_{02} = 4.72$ kPa	mat1
Samani *et al.*[26]	Linear elastic		$E = 3.25 \pm 0.9$ kPa at 5% strain	mat2
Tanner *et al.*[30]	Linear elastic (MM1)		$E = 1$ kPa	
	Hyper-elastic Neo-Hookean (MM1nH)		$C_{10} = 0.13$ kPa	mat3
	Piecewise-linear & exponential elastic (MM7)	*Ex vivo* based on Azar *et al.*[3]	$= 718.16\varepsilon + 4.46$ if $0 \leq \varepsilon$<0.25 $= 184$ if $\varepsilon \geq 0.25$	
	Hyper-elastic Neo-Hookean (MM7nH)		$C_{10} = 19.8$ kPa	mat4
	Hyper-elastic Mooney-Rivlin (MM7MR)		$C_{10} = 46.42$ kPa $C_{01} = -31.77$ kPa $C_{20} = 37.07$ kPa $C_{11} = 1.96$ kPa $C_{02} = 1.51$ kPa	mat5
	Linear elastic (MM8)	*Ex vivo* based on Krouskop *et al.*[14]	$E = 18.5$ kPa	
	Hyper-elastic Neo-Hookean (MM8nH)		$C_{10} = 2.4$ kPa	mat6
	Hyper-elastic Mooney-Rivlin (MM8MR)		$C_{10} = 5.83$ kPa $C_{01} = -3.14$ kPa $C_{20} = 0.9$ kPa $C_{11} = 0.64$ kPa $C_{02} = 0.08$ kPa	mat7
	Polynomial elastic (MM9)	*Ex vivo* based on Samani *et al.*[24]	$E = 519.7\varepsilon^2 + 2.4\varepsilon + 4.9$	
	Hyper-elastic Neo-Hookean (MM9nH)		$C_{10} = 3.6$ kPa	mat8
	Hyper-elastic Mooney-Rivlin (MM9MR)		$C_{10} = 10.0$ kPa $C_{01} = -7.14$ kPa $C_{20} = 3.12$ kPa $C_{11} = 1.82$ kPa $C_{02} = 2.07$ kPa	mat9

TABLE 1. continued.

Lead author	Constitutive model	Experimental condition	Material constants	Material model no. in our study
Del Palomar *et al.*[5]	Hyper-elastic Neo-Hookean	*In vivo* gravity loading	$C_{10} = 3.0$ kPa	mat10
Rajagopal *et al.*[21]	Hyper-elastic Neo-Hookean	*In vivo* gravity loading	$C_{10} = 0.08$ kPa	mat11
			$C_{10} = 0.13$ kPa	Same as mat3
Lapuebla-Ferri *et al.*[15]	Hyper-elastic Neo-Hookean	*Ex vivo* based on Samani *et al.*[26]	$C_{10} = 0.54$ kPa	mat12

(Materialise Inc., Leuven, Belgium) to semi automatically segment the different relevant anatomical regions of interest for the simulation study (see Fig. 2).

The bony thoracic wall was modelled as a continuous surface including the intercostal muscles and was assumed to completely restrain displacements as the posterior demarcation of the deformable model. Fat and glandular tissue as well as the pectoral muscles and the skin were summarized as one component in the segmentation (see Fig. 2). Fat and gland were considered as homogenous material for FE simulation as previous studies found the mechanical properties of fibro glandular and fat tissue to be in comparable magnitude.[5,15,21,23,26,30] The mechanical properties of the skin and muscle are not taken into account in this study. The pectoral muscles are segmented into one single compartment and we did not distinguish between the major and minor pectoral muscles. Since all anisotropic material behaviours are neglected in this study, fibre directions that differ in the two muscular parts are not relevant here. The material model used to describe the deformability of the muscular tissue is treated as being similar to that of the overall breast soft tissue, as our preliminary study showed no relevant influence of varying boundary conditions (muscle included vs. muscle excluded) on the simulation accuracy compared to the variation of material parameters.[19] Thus the employed material models have to be considered as an overall representation of the soft tissue of the breast containing the properties of gland, fat, muscle as well as skin.

The segmented surfaces were post-processed in an adequate 3-D surface processing software (Geomagic Studio 12®, Raindrop Geomagic, Inc., NC, USA) to improve the surface quality and reduce segmentation artefacts that could disturb later mesh generation. Triangulated surfaces prepared in this manner can be utilized for the division of the complex anatomical shapes into FEs, e.g., a multitude of simplistic shapes that can be computed easily. For the generation of the FE model the meshing software ICEM (Ansys Inc., Canonsburg, PA, USA) has been applied. Two surfaces containing the thoracic wall and the soft tissue of the breast as an entire component were imported to ICEM in triangulated STL format. In order to eliminate the irrelevant parts of the breast model for the FE simulations (e.g., the shoulders), a box was defined to demarcate the model. The lateral demarcations have been set to exclude the arms. As posterior cut off, the location of the maximal extension of the thorax in lateral extension is defined. The upper demarcation is defined as the cranial borders of the clavicle, while the lower border is placed 10 cm below the breast to exclude potential influences of the system boundary conditions to the soft tissue deformation of the breast (see Fig. 2).

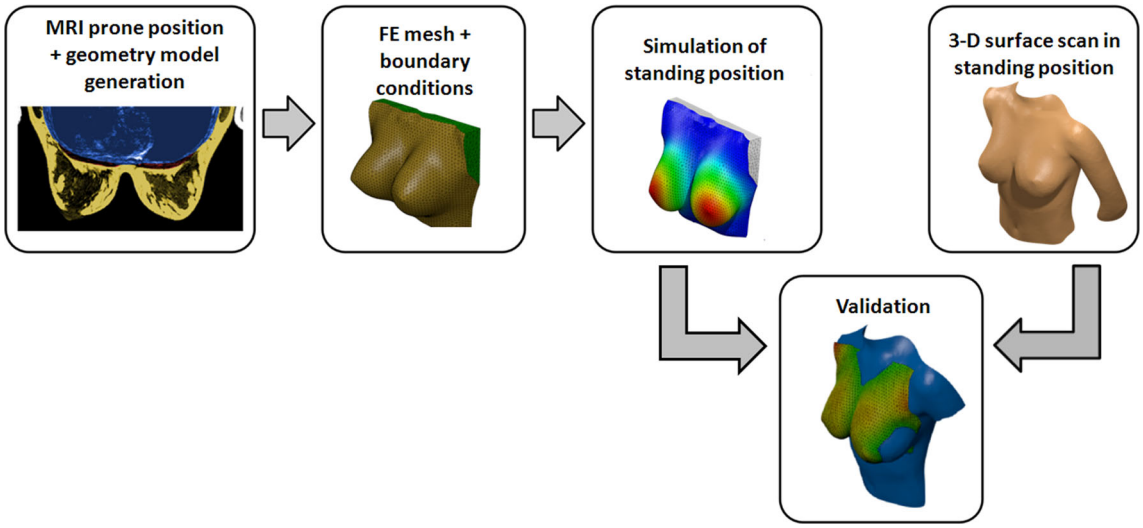

FIGURE 1. An overview of the developed workflow to simulate and analysis 3-D breast deformations: starting with the MRI data acquisition and segmentation of the relevant anatomical components from MRI prone position for the generation of a realistic model geometry over the FE mesh generation and definition of boundary conditions to the FE simulation of the standing position and the final validation of the simulation by comparing the resulting breast surface displacement to the real breast geometry using corresponding 3-D surface scans.

Boolean operations were used to create the intersection surfaces between the different segmented anatomical regions. Thus, any initial penetrations between the different parts are avoided which may otherwise cause problems of convergence of the FE analysis. TCL/TK scripting was used in ICEM to implement a routine automation of the whole mesh generation procedure. This process delivered standardized and suitable meshes for FE analysing with uniform mesh density for each test person. The different parts of the model (skin/fat/gland/muscle and thoracic wall) are connected to each other through shared nodes allowing no sliding between the two compartments. Self-contact at skin level was not modelled in these simulations because manual evaluations performed in previous work showed only negligible penetrations even in patients with large breast volume.

For the simulation, tetrahedron solid elements were used with up mixed formulation and an enhanced hydrostatic pressure.[15] This theoretical element formulation is suitable for modelling irregular meshes and general material formulations (including incompressible materials) as well as the consideration of large deformations and rotations according to the used finite strain theory. The programming language Ansys Parametric Design Language (APDL) was used for implementation and automating the whole process of the following FE simulation that has been performed with ANSYS (Ansys Inc., Canonsburg, PA, USA). The models are displacement converged and we used the convergence control from ANSYS (CNVTOL) with a default tolerance value for displacement for a nonlinear analysis of 0.05 (5%) considering the solver checking as sufficient.

Boundary Conditions

The above described upper, lower, and lateral demarcations of the FE geometry model have been considered as fixed boundaries, i.e., all FE nodes at these locations are kept initially fixed. Furthermore the nodes corresponding to the bony thoracic wall representing the dorsal demarcation of the simulation model can be considered as being completely rigid in comparison to the overlying soft tissues and therefore fixed displacement boundary conditions were imposed in this area (see Fig. 2).

Iterative Algorithm for the Calculation of an Unloaded Reference State

Due to the soft constitution of the tissue, the breast is largely deformed even if except gravity no other loads are acting. Therefore, all possible spatial positions of the test person yield a deformed geometry of the breast since gravity effects cannot be excluded easily. For mechanical simulations however, an unloaded state of the geometries is needed as the starting point of the simulation. Since when exceeding the linear Hookean domain, it is not possible to simply using an acquired deformed state as the starting configuration that is treated as being unloaded because the material properties in the stress free state are different from those under loading. Calculating the non-deformed reference state out of a known deformed

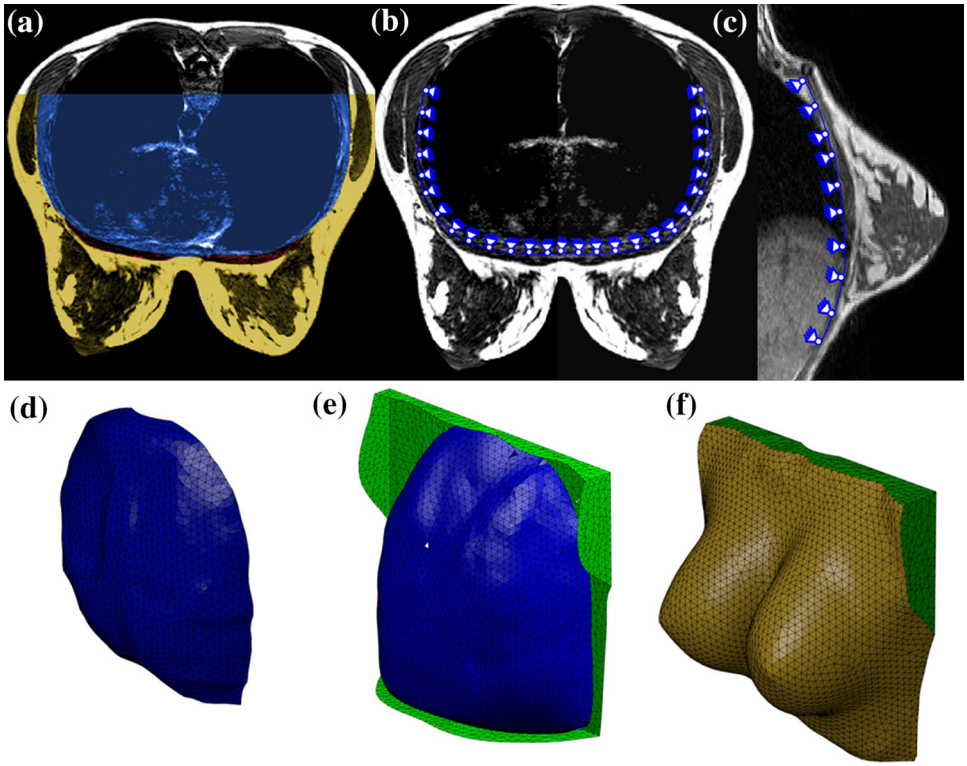

FIGURE 2. MRI data acquisition in gravity-loaded prone position with segmentation of the relevant anatomic breast region summarizing skin, fat, gland, and muscle as one compartment and the thoracic wall (a). The investigated dorsal boundary condition: the thoracic wall is considered to be the dorsal delimitation of the model in horizontal (b) and sagittal (c) views. The corresponding finite element mesh, consisting of the thoracic wall (d), the lateral, cranial and caudal system boundaries (e), and the overlying breast soft tissue (f).

configuration can be classified as an inverse problem. Due to the high deformation and the hyper-elastic material behaviour, a simple recalculation with inverse gravity has shown not to be satisfyingly accurate. Previous studies did not consider these effects and used a single step method instead,[5] but recently, more advanced investigations on this subject have been conducted taking into account these influences.[15,17] Rajagopal *et al.*[15] presented an inverse algorithm for breast soft tissue simulation to address this topic. The here described approach uses a similar method for the iterative calculation of the unloaded reference state.

In this heuristic approach, an estimation of the non-deformed configuration ($\mathbf{X}$) is made based in the segmented deformed configuration ($\mathbf{x}_{\mathrm{MRI}}$) derived from MRI. A first approximation of the non-deformed configuration $\mathbf{X}_0$ is made by a one-step backward calculation (inverse prone gravity) using $\mathbf{x}_{\mathrm{MRI}}$ as a starting configuration with $\mathbf{K}_{\mathrm{MRI}}(\mathbf{x}_{\mathrm{MRI}},\mathbf{u})$ being the non-linear system stiffness matrix in that state and $\mathbf{f}_0$ being the vector of body loads due to gravity:

$$\mathbf{K}(\mathbf{x}_{\mathrm{MRI}},\mathbf{u})\mathbf{u}_{\mathrm{inv}} = -\mathbf{f}_0.$$

This equation has to be solved to access the displacement vector $\mathbf{u}_0$ that is denoting the displacement between the two states and allows for a calculation of a first approximation of the undeformed state:

$$\mathbf{X}_0 = \mathbf{x}_{\mathrm{MRI}} + \mathbf{u}_{\mathrm{inv}}.$$

The subsequent procedure to improve this estimate may be performed multiple times in an iterative loop, see Fig. 3 visual representative. To check the validity of this estimation of the non-deformed configuration, we may use $\mathbf{X}_0$ as a starting geometry of a new (forward) calculation with prone gravity as boundary condition ($n = 0$ in the first iteration):

$$\mathbf{K}(\mathbf{X}_n,\mathbf{u})\mathbf{u}_n = \mathbf{f}(\mathbf{X}_n).$$

is solved for $\mathbf{u}_n$ with regular FE approach and hence a calculated shape of the breast loaded by prone geometry can be deducted:

$$\mathbf{x}_n = \mathbf{X}_n + \mathbf{u}_n.$$

This resulting $\mathbf{x}_n$ may be compared to the initially acquired geometry $\mathbf{x}_{\mathrm{MRI}}$:

$$\mathbf{u}_{\mathrm{dev},n} = \mathbf{x}_{\mathrm{MRI}} - \mathbf{x}_n.$$

The deviations between these two states $\mathbf{u}_{\mathrm{dev},n}$ can be used as displacement boundary conditions on the

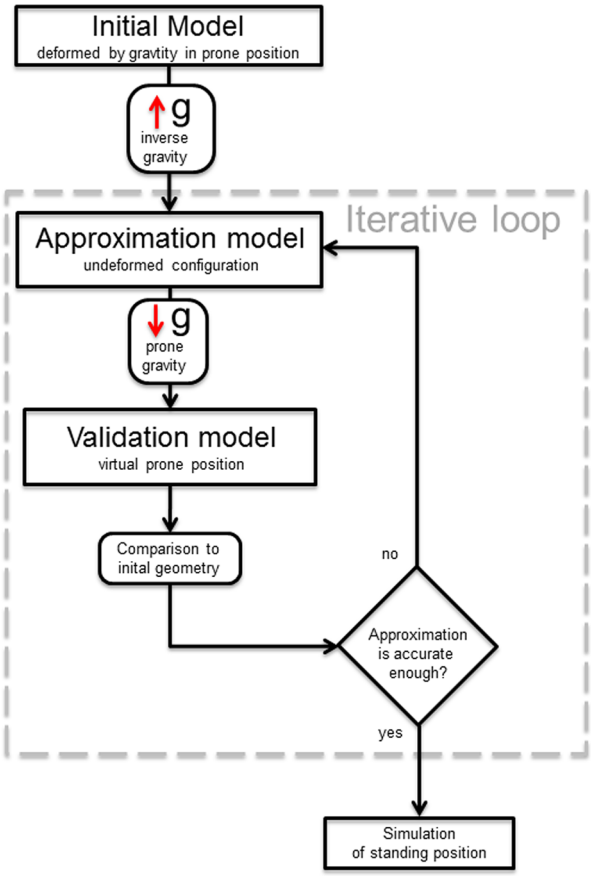

FIGURE 3. Workflow of the heuristic iterative procedure that is used to solve the inverse problem of calculating the undeformed state on the basis of a known gravity deformed state.

current deformed geometry $\mathbf{x}_n$ and solved for reaction forces $\mathbf{f}_{\text{corr},n}$:

$$\mathbf{K}(\mathbf{x}_n)\mathbf{u}_{\text{dev},n} = \mathbf{f}_{\text{corr},n}.$$

The resulting reaction forces $\mathbf{f}_{\text{corr},n}$ derived from this FEM simulation are needed to change the estimated deformed configuration $\mathbf{x}_n$ to match the real deformation $\mathbf{x}_{\text{MRI}}$. These reaction forces are then transformed to the current estimate of the undeformed configuration $\mathbf{X}_n$ to get a better approximation of the real undeformed state:

$$\mathbf{K}(\mathbf{X}_n)\mathbf{u}_{\text{corr},n} = \mathbf{f}_{\text{corr},n}.$$

With the correction vector $\mathbf{u}_{\text{corr},n}$ applied to the current estimation $\mathbf{X}_n$ a better estimation may be calculated with

$$\mathbf{X}_{n+1} = \mathbf{X}_n + \mathbf{u}_{\text{corr},n}.$$

This new estimate $\mathbf{X}_{n+1}$ may be used in a new forward calculation to evaluate its accuracy and if necessary a new loop of improvements may be performed.

To avoid unnecessary computations, a stop criterion was implemented as follows: if the difference between two consecutive iterations $\mathbf{u}_{\text{corr},n}$ and $\mathbf{u}_{\text{corr},n+1}$ is less than 5% of the difference at the first iteration $\mathbf{u}_{\text{corr},1}$, the unloaded model is considered as satisfyingly accurate and the loop is exited.

The presented approach may not guarantee convergence for all meshes and arbitrarily large deformations. If the difference between the deformed and undeformed states are too large the inherent error of the method that is made by the simple transformation of $\mathbf{f}_{\text{corr},n}$ between the different states $\mathbf{x}_n$ and $\mathbf{X}_n$ is dominant leading to divergence of displacements.

Applied Constitutive Breast Models

Different material constants are suggested by several authors for the biomechanical modeling of breast soft tissue mechanics, such as linear elastic, piecewise-linear elastic, exponential elastic, and different hyper-elastic constitutive models (see Table 1). Krouskop *et al.*,[14] Wellman *et al.*[32] and Samani *et al.*[25,26] obtained the material parameter based on *ex vivo* indentation tests. Azar *et al.*[3,4] applied the same material model as Wellman *et al.*,[32] but suggested a corrected stress–strain relationship for more than 15.5% strain. Samani *et al.*[24] used a polynomial elastic material model to approximate Wellman's stress–strain relationship. Tanner *et al.*[30] created Neo-Hookean and Mooney-Rivlin hyper-elastic models (called MM7nH, MM8nH, MM9nH, MM7MR, MM8MR, MM9MR) in accordance to the previously reported values by Azar *et al.*,[3,4] Krouskop *et al.*[14] and Samani *et al.*[24] (see Table 1). Recently, Lapuebla-Ferri *et al.*[15] used a Neo-Hookean constitutive model to extend the linear elastic moduli based on the measurements of Samani *et al.*[26] Del Palomar *et al.*[5] and Rajagopal *et al.*[20,22] obtained the material parameters for Neo-Hookean material model based on *in vivo* gravity loading. Linear elastic material models, as used by Tanner *et al.*[29] are from a biomechanical point of view expected not to be deformable enough to describe the deformations of the breast tissue and even if only gravity loading is applied the strains exceed the Hookean domain of linear stress–strain relationship.[19] Thus it is necessary to use hyper-elastic material formulations to describe the deformations of the breast with FE simulations. However, we applied one linear elastic material model as a reference to eventually gain further insight in the system behavior of our simulation models.

Out of the above described constitutive models in Table 1, 12 different constitutive material models (called mat1–12) were chosen for comparison in the scope of this study that covered the range of published stress–strain relationships. In our simulations, all

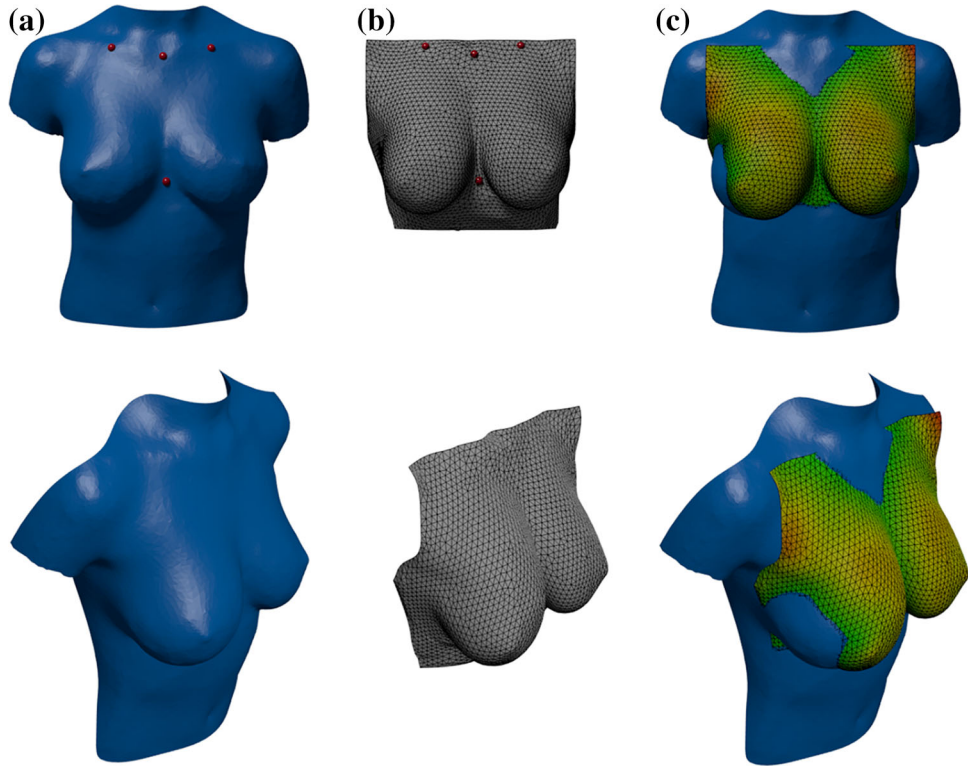

FIGURE 4. 3-D surface scan of a test person in standing position (a) and corresponding participants FE simulated breast model in upright position (b) calculated from the MRI based geometry in prone position with relevant landmarks for data registration in space. 3-D comparison between the FE breast simulation results and the real participant's breast geometry (c) acquired by 3-D surface imaging data calculating the mean surface difference between the superimposed models using the root-mean-square (mm) node to surface integration (above and below, right).

hyper-elastic material models are considered to be incompressible.

Validation of Simulation Results

To determine the accuracy of the FE simulation for different material models, the surface distances (mm) between the FE breast simulation results in upright position and the real breast geometry obtained by 3-D surface imaging data was calculated for each volunteer. The skin surface of the simulated 3-D breasts is exported as a triangulated surface and superimposed onto the real 3-D breast surface scans (see Fig. 4), similar to the validation method introduced by Del Palomar *et al.*[5] for the total breast region. A landmark-based data registration is performed to guarantee that both surfaces are positioned accordingly in one common coordinate system using only bony landmarks as the sternal notch, the left and right clavicle and the xiphoid tip (see Fig. 4) as these landmarks remain relatively stable during the simulation of the soft tissue deformation. A self-developed software routine in C++ was implemented to calculate the distance between the superimposed models with an algorithm that uses node to surface root mean square integration of the Hausdorff distance in mm, according to Aspert *et al.*[2] The whole procedure is automated in batch mode to overcome cumbersome manual comparisons and to avoid any examiner variability.

Furthermore, a more detailed analysis was performed to analyse the performance of the simulation models according to all clinical relevant regions of the breast. The breast was marked according to a previously described and validated measurement protocol[6,11,12]: approximately 1 cm beside the sternal notch along the sternum to the medial breast fold, following the submammary fold to the lateral breast fold, along the frontal axillary fold and the lateral offshoot of the pectoral muscle up to below the clavicle and back to the sternal notch. This selected breast region is further divided in four clinically established breast quadrants (red = upper inner quadrant, green = lower inner quadrant, blue = lower outer quadrant, and yellow = upper outer quadrant) according to our previously standardized and validated approach (Fig. 5, right).[7] Again the surface distances (mm) between the two superimposed models was calculated for each volunteer using the node to surface root mean square integration of the Hausdorff distance in mm, according to Aspert *et al.*[2]

Because the two above described evaluation methods do not provide any information about the algebraic sign of the deviation between the two superimposed models solely based on the root mean square calculations, i.e., it is not possible to determine whether a tested material model is too stiff or too soft. Therefore, a third evaluation was performed. In this approach anatomical landmarks are placed on the sternal notch and on the right and left nipple of each breast on the 3-D surface scan as well as on the FE breast simulation results. The Euclidean distances from sternal notch to left and right nipple are calculated and averaged for all models providing one parameter for validation. The deviation between the measured sternal notch to nipple distances on both models was calculated for all the applied material models, expressed as the absolute difference in mm.

The simulation results for the different constitutive models investigated in this study are compared and statistically evaluated. The Wilcoxon rank-sum test was used to test for significance of the comparisons of different literature references. For all tests a two-tailed global significance level of $p < 0.01$ was utilized. GNU Octave (www.gnu.org/software/octave) was used for the data processing and plotting of the results. Mean, standard deviation (SD), maximum (MAX), minimum (MIN), median values as well as quantile partitions were obtained for all breast surface comparisons in mm.

RESULTS

The iterative algorithm is applied to the deformation of the breast under gravity load in prone position and the calculation of an unloaded configuration. Convergence of the presented simulation algorithm cannot be guaranteed for every participant: non-convergence (n.c.) was observed 12 times (mat2: 1 × n.c.; mat3: 2 × n.c.; mat11: 9 × n.c). However, with 94.4% (204 of 216) converged solutions, the algorithm can be classified as robust.

An overview of all comparisons between FE simulation results for the standing position and the 3-D surface images as references for the total breast region are given in Table 2. All deviations are listed as integrated mean over the surface (mm). Mean values and standard deviations as well as minimal and maximal values for all investigated material parameter sets are listed. A graphical representation of this data is shown in Fig. 6. The box plots show the median values as well as the first and third quartile while the whiskers are denoting the maximal and minimal values. The simulation accuracy with a mean difference of 7.40 ± 1.70 mm (range 4.61–9.85) for mat3 and 7.33 ± 1.48 mm (range 5.81–9.36) for mat11 demonstrate an obvious advantage compared to the other material models ($p < 0.01$; only comparisons of mat5 to mat11 and mat12 show p-values of 0.0121 and 0.0103, respectively). By comparing mat3 to mat11, no significant difference between the two models is detectable ($p = 0.89$). However, mat11 shows inferior convergence behaviour with 9 converged simulations out of 18 performed. Furthermore, no significant differences in the comparison between all other material models are apparent ($p > 0.01$).

The additionally performed evaluations according to the clinical breast quadrants show that there are significant differences between the regions of the breast, as visualized as mean deviations for each

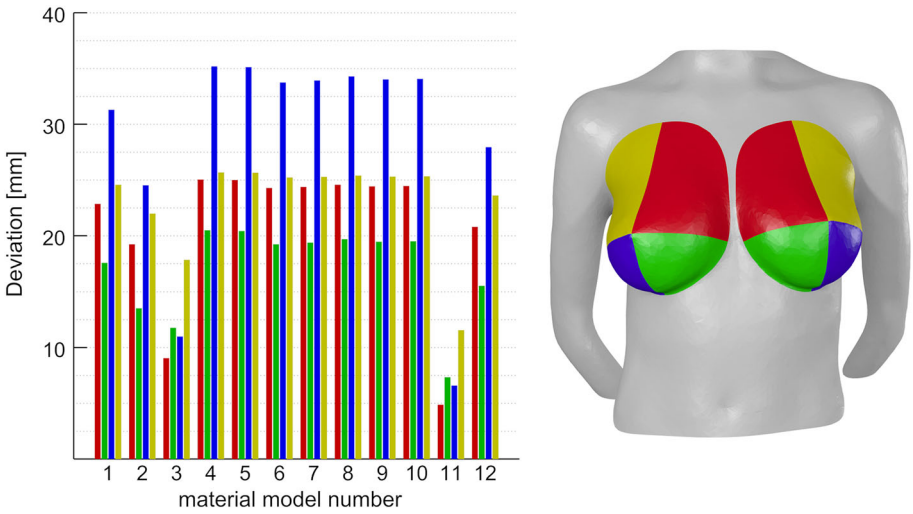

FIGURE 5. 3-D breast surface comparison between the FE breast simulation and the 3-D breast scan according to the clinical relevant breast quadrants (right) using the root-mean-square (mm) node to surface integration. Mean values over all volunteers are visualized for each tested material and each breast quadrant (left).

TABLE 2. Comparison of the surface distances between the FE breast simulation results and the real breast geometry obtained by 3-D surface imaging data for each investigated material model and each test person using root-mean-square values (mm).

Volunteer No	Samani MR mat1	Samani E mat2	Tanner MM1nH mat3	Tanner MM7nH mat4	Tanner MM7MR mat5	Tanner MM8nH mat6	Tanner MM8MR mat7	Tanner MM9nH mat8	Tanner MM9MR mat9	Del Palomar nH mat10	Rajagopal nH mat11	Lapuebla-Ferri nH mat12
1	10.51	9.50	n.c.	11.69	11.66	11.18	11.23	11.37	11.26	11.29	n.c.	9.49
2	12.75	12.29	9.85	13.39	13.37	13.15	13.18	13.24	13.19	13.21	9.36	12.29
3	14.80	13.83	9.65	16.14	16.12	15.63	15.68	15.82	15.72	15.74	n.c.	13.83
4	16.52	n.c.	n.c.	18.36	18.31	17.52	17.62	17.83	17.67	17.71	n.c.	14.78
5	8.03	7.39	5.03	8.99	8.98	8.63	8.67	8.77	8.70	8.71	5.84	7.39
6	8.92	7.93	5.92	10.14	10.11	9.65	9.71	9.83	9.73	9.76	n.c.	7.92
7	11.64	10.88	8.45	12.69	12.67	12.28	12.33	12.43	12.35	12.37	n.c.	10.90
8	6.88	6.56	5.44	7.42	7.41	7.23	7.25	7.30	7.26	7.27	5.81	6.55
9	12.75	11.89	8.83	13.94	13.91	13.46	13.52	13.64	13.55	13.57	n.c.	11.89
10	10.08	9.90	8.89	10.37	10.37	10.27	10.28	10.31	10.29	10.29	8.45	9.91
11	9.97	9.81	8.93	10.23	10.23	10.14	10.15	10.18	10.16	10.16	8.69	9.81
12	8.98	8.58	6.72	9.59	9.58	9.36	9.39	9.45	9.40	9.41	n.c.	8.57
13	6.95	6.91	6.63	7.05	7.05	7.02	7.02	7.03	7.03	7.03	n.c.	6.92
14	7.55	7.43	6.60	7.77	7.76	7.70	7.71	7.72	7.71	7.71	6.24	7.44
15	9.74	9.34	7.01	10.39	10.38	10.16	10.19	10.25	10.20	10.21	6.29	9.33
16	9.14	8.33	4.61	10.22	10.20	9.80	9.85	9.96	9.87	9.89	n.c.	8.31
17	8.87	8.60	6.81	9.35	9.35	9.20	9.22	9.26	9.22	9.23	6.32	8.60
18	11.11	10.73	9.08	11.64	11.63	11.43	11.46	11.51	11.47	11.48	8.92	10.75
Mean	10.29	9.41	7.40	11.08	11.06	10.77	10.80	10.88	10.82	10.84	7.33	9.70
SD	2.62	2.02	1.70	2.96	2.95	2.80	2.82	2.86	2.83	2.83	1.48	2.34
Max	16.52	13.83	9.85	18.36	18.31	17.52	17.62	17.83	17.67	17.71	9.36	14.78
Min	6.88	6.56	4.61	7.05	7.05	7.02	7.02	7.03	7.03	7.03	5.81	6.55

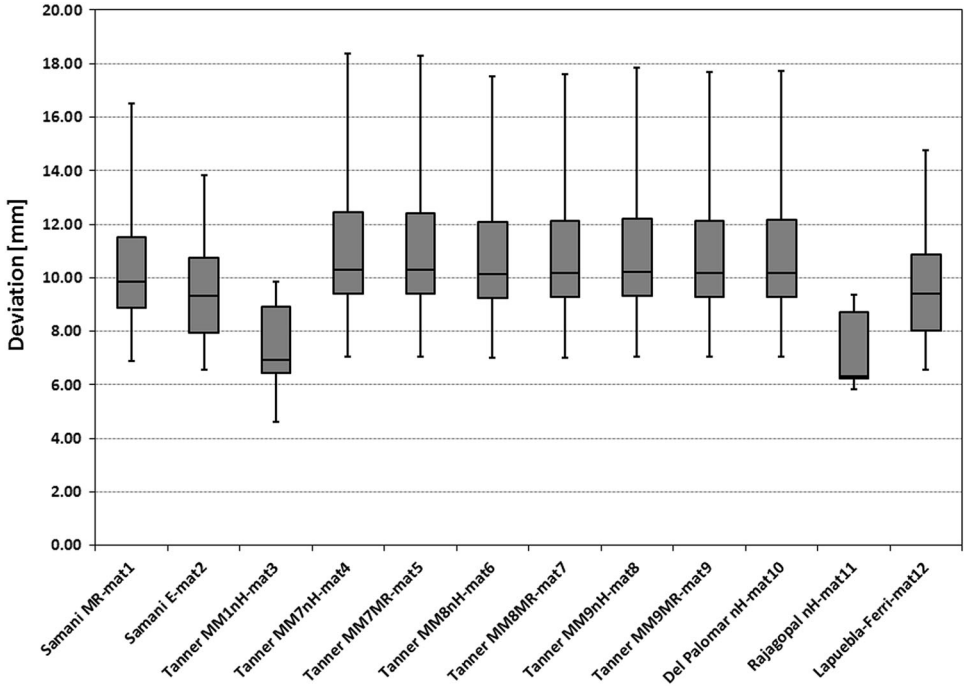

FIGURE 6. Comparison of the simulation accuracy of the investigated material models expressed as the surface distances (mm) between the FE breast simulation results and the real breast geometry obtained by 3-D surface imaging data for each volunteer for the total breast region. The box plots show the median values as well as the first and third quartile while the whiskers are denoting the maximal and minimal values.

material model and each breast quadrant (Fig. 5, left). Evaluating the differences equally over all utilized material models, the best accordance with the 3-D surface scan could be found for the lower inner quadrant followed by the upper inner quadrant and the upper outer quadrant. The worst accordance was found for the lower outer quadrant; comparisons between all four quadrants reveal highly significant differences ($p < 0.001$). The comparison according to the different material models illustrates once again that mat3 and mat11 perform significantly better ($p < 0.01$) than the other models (Fig. 5, left). In general, no relevant differences between the breast quadrant analysis (Fig. 5) and the total breast comparison (Fig. 6) are detected.

The distance analysis between the sternal notch and nipples shows an outcome comparable to the previously performed evaluations (see Fig. 7). Again, mat3 and mat11 are significantly closer to the distances measured in the 3-D surface scans compared to the other material models. Between mat3 and mat11 no statistically significant advantage of either model could be found ($p > 0.01$). However this evaluation shows that mat11 is more often too soft, hence overestimating the real distance (mean value −5.65 mm), while mat3 (mean 7.45 mm) is too stiff yielding too short sternal notch to nipple distances, just like all the other material models (Fig. 7).

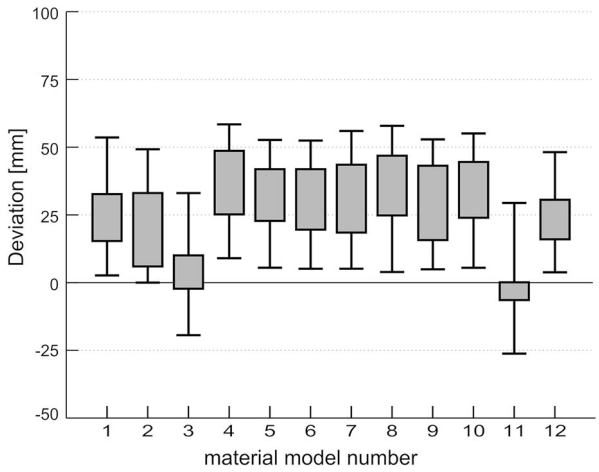

FIGURE 7. Comparison of the deviation between the measured sternal notch to nipple distances on the 3-D surface reference model and the FE breast simulation results expressed as the absolute difference in mm for all the applied material models.

DISCUSSION

According to our findings, many of the material parameters proposed in the literature treat the soft tissue as too stiff, i.e., permitting not enough deformation due to gravity loading. The group of relatively stiff material parameters includes those derived by

mono-axial tension tests and indentations tests.[14,25,32] The group of these material models does not allow enough deformation of the soft tissue to represent the real behaviour of the breast's soft tissue.

In our study, mat3 proposed by Tanner *et al.*,[30] and mat11 by Rajagopal *et al.*[21] have proven to be best suited material models to describe the overall mechanical behavior of the breast under gravity loading out of the investigated material parameter sets (see Figs. 5–7; Table 2). However, between these two models, no significant difference was observed.

In general, no relevant differences between the breast quadrant analysis (Fig. 5) and the total breast comparison (Fig. 6) are detected. This finding is true for the fully automated comparison of the total breast region as well as for the comparisons according to the four breast quadrants, as no relevant differences between the methods are apparent. The latter evaluation method allows for a more detailed evaluation of the local accuracy of the simulation and we may conclude that the surface is especially well captured at the two inner quadrants while there is in general significantly more deviation in the outer quadrants. For the daily clinical routine this might be of high relevance as nearly 48% of the primary tumors are located in the upper outer quadrant. Therefore, further clinical studies are needed to evaluate the reliability of the presented biomechanical breast models in clinical practice to predict the movement of tumors during different imaging procedures and to evaluate the accuracy of tumor tracking according to the different breast quadrants in relation to the applied diagnostic modality. Several recent studies are very promising by applying biomechanical FE models using patient specific parameter optimization *in vivo*, semi-automatic segmentation methods for tissue classification, fully automated FE mesh generation and by applying fully automated registration algorithms of volume images with 2-D mammograms in the field of clinical tumor diagnostic with a mean target registration error range of 9–13 mm.[8,10,16,17]

A comparison of the calculated sternal notch to nipple distance showed that mat3 is prone to underestimate the deformation while in contrast mat11 is rather overestimating it (Fig. 7). Hence, we may conclude that the set of material parameters that is best suited to describe the mean material behavior of all subjects included in our study lies in between these two proposed material stiffnesses. Both of these models use a Neo-Hookean model as theoretical constitutive formulation. The use of such hyper-elastic models is inevitable because of the large deformations that the breast tissue undergoes under gravity loading. Hence, from a biomechanical point of view one would expect that the linear elastic model (mat2) used in our study as a reference will deliver worse results. However, an interesting finding of this study is the fact that there are stiffer hyper-elastic material formulations proposed in literature that allow even less deformations making the results of the linear elastic simulations not the worst of all conducted simulations.

None of the utilized material models was capable of delivering surface accuracy in the sub-millimeter range. These results look at first glance to be relatively bad, however it has to be kept in mind that the surface deviations are measured on the whole surface area of the simulation model including the region of the shoulders where the difference in initial positioning of the volunteers have shown to influence the simulation accuracy mostly. For the upright 3-D surface scans the subjects were asked to cross their arms behind the back, while in the MRI acquisition in prone position the subjects had to lay comfort on the individual pillow support with arms by the side. These differences in positioning cannot be captured by the simulation approach that is used here. An evaluation that is focused on the breast region solely delivers better accordance (see Fig. 5). However, the shortcoming of the breast quadrant evaluation is the observer interaction that is necessary to define the breast contours manually. The difference between both evaluations is only a shift in absolute values. As expected no changes in the comparisons between the material models was investigated.

However, one additional shortcoming of the study is that the two best working material models did not yield simulation results for all calculations. The relatively soft material behavior leads to high strains and thus numerical instabilities are more likely to arise, than for stiffer material formulations. Therefore, the need of an improvement of the inverse routine's robustness in the domain of large strains remains. Another possible cause of these convergence issues are the utilized constitutive material formulations themselves: other exponential material formulations, e.g., those proposed by Holzapfel *et al.*[9] may provide more numerical stability to these calculations. Furthermore, it has been recognized that breast size had an essential impact on convergence behavior: the larger the breast size, the more likely non-convergence of the calculation occur due to excessive deformations.

Tanner *et al.*[30] and Rajagopal *et al.*[21] used an approach similar to our study with *in vivo* calculation of gravity. In our opinion these methods are well suited for the determination of human soft tissue material parameters, because they can overcome the inherent limitations of all *ex vivo* material tests that have to deal with the unclear changes in mechanical properties of the tissue after extraction. Furthermore, the clinical application for the acquisition of patient specific

material properties is easier to realize with non-invasive approaches.

Therefore, we intend to leave the subject of applying preliminarily defined material parameters in future studies by extending the solution space in an optimization process. With the presented automatic workflow, it is possible to perform numerous calculations with minimal additional effort. So it seems possible, that these parameter optimizations can be performed for different patients and may provide patient individually adjusted material parameter sets in the near future. Recent studies by our research group in this field are underway to non-invasively determine constitutive material parameters for the different anatomical compartments of the female breast by simulating the breast deformation using MR images at different loading conditions solely. The thus gained information can be used for the development of accurate simulations for oncologic tumor detection across multiple image patterns procedures including non-rigid multimodal image registration or in surgical planning, i.e., in tumor ablation surgery and subsequent breast reconstructions with autologous tissue transplants.

The level of abstraction in the models utilized in this study is relatively high, following our intention to focus on the mechanical behavior of one specific anatomical region. Neglecting the potential influence of additional pectoral muscle deformations enabled a feasible constitutive breast model comparison in the presented work. However, a more complex anatomical model of the breast, i.e., with subdivision of the model in skin components, fat and fibro-glandular tissues as well as muscle tissue modeled with different material parameters, might provide an even better matching of accordance between simulation results and surface scanned data. For these models, the mechanical properties of skin and muscle with its anisotropic behavior could also be included in the simulations. Considering these parts with separate constitutive models, the dimensionality of the problem increases rapidly, needing a larger number of additional simulations. Since the aim of the present study was to evaluate and compare the reported material models for breast soft tissue, we decided not to model the muscle and skin material as separate compartments.

As deformation accuracy and computation time are the two main constraints for the modeling of soft tissues, the required accuracy level depends on the medical application and the needed level of detail.[22] Tumor tracking over different time points must be very precise and accurate to fulfill oncology requirements resulting in larger computation time. Essential biomechanical requirements have to be fulfilled to enable realistic breast soft tissue simulations considering an accurate geometric breast model, correct breast boundary and loading conditions, a reliable constitutive breast model and accurate biomechanical breast parameters.[22] The reliability of these essential biomechanical key parameters determines the simulation accuracy.

The ideal conception of a successful medical simulation is only partly convertible because of technical practicability and limitations to the above named complex biomechanical requirements. However, for a patient specific prediction of suspicious lesions movement during different imaging procedures, clinical tumor tracking by integrating comparison of multimodality images into the simulation model or planning breast reconstruction surgery with large soft tissue deformation, more reliable biomechanical breast models must be developed in the future to ensure a very high degree of adaptation to specific medical simulation applications.

From this manuscript we may conclude that the approaches introduced in this paper permit the simulation of soft tissue deformation of the breast under *in vivo* gravity loading using an iterative calculation of the unloaded reference state of the breast. The methods showed their applicability with different material properties for breast soft tissue and simulations results were comparable to corresponding 3-D surface scans. Our simulation method has the advantage that it is fully automated after the required geometric modeling and does neither require a time consuming training nor any cumbersome manual interaction avoiding examiner variability. In addition, our non-invasive approach presents an attractive alternative to existing testing methods for the determination of human soft tissue material parameters.[28]

Finally, our study demonstrated that Neo-Hookean hyper-elastic models proposed by Tanner *et al.*[30] and Rajagopal *et al.*[21] represents the most appropriate method to describe the overall mechanical behavior of the breast under gravity loading out of the investigated group of material parameters.

ACKNOWLEDGMENTS

The authors would like to thank Prof. Dr. A. Haase, Director of the Institute of Medical Engineering at the Technische Universität München (IMETUM), Germany for his cooperation and infrastructural support. Furthermore, the authors are grateful to Prof. Dr. E. J. Rummeny, Director of the Institute of Radiology and Interventional Radiology, Klinikum rechts der Isar, Technische Universität München for his cooperation and infrastructural support, which contributed enormously to the realization and success of this study.

Funding for the study was received by the Federal Ministry of Economics and Technology (BMWi-Funding No. 16INO607).

CONFLICT OF INTEREST

All authors disclose any financial or commercial associations and personal relationships with other people, organisations or with the companies named in the study that would inappropriately influence (bias) their work or create a conflict of interest with information presented in the submitted study. None of the authors are shareholders of one of the named companies whose hard- and software products were used in the study.

REFERENCES

[1]American Cancer Society, Breast Cancer Facts & Figures 2011–2012. http://www.cancer.org/acs/groups/content/@epidemiologysurveilance/documents/document/acspc-030975.pdf. Accessed 29 July 2013.

[2]Aspert, N., D. Santa-Cruz, and T. Ebrahimi. Mesh: measuring errors between surfaces using the Hausdorff distance. In: Proceedings of the IEEE International Conference on Multimedia and Expo, Lausanne, Switzerland, 2002, pp. 705–708.

[3]Azar, F., D. Metaxas, and M. Schnall. A deformable finite element model of the breast for predicting mechanical deformations under external perturbations. *Acad. Radiol.* 8:965–975, 2001.

[4]Azar, F., D. Metaxas, and M. Schnall. Methods for modeling and predicting mechanical deformations of the breast under external perturbations. *Med. Image Anal.* 6:1–27, 2002.

[5]Del Palomar, A., B. Calvo, J. Herrero, J. Lopez, and M. Doblare. A finite element model to accurately predict real deformations of the breast. *Med. Eng. Phys.* 30:1089–1097, 2008.

[6]Eder, M., A. Schneider, H. Feussner, A. Zimmermann, C. Hoehnke, N. Papadopulos, and L. Kovacs. Breast volume assessment based on 3D surface geometry: verification of the method using MR imaging. *Biomed. Tech.* 53:112–121, 2008.

[7]Eder, M., F. von Waldenfels, A. Swobodnik, M. Klöppel, A. K. Pape, T. Schuster, S. Raith, E. Kitzler, N. Papadopulos, H. G. Machens, and L. Kovacs. Objective breast symmetry evaluation using 3-D surface imaging. *Breast* 21:152–158, 2012.

[8]Han, L., J. H. Hipwell, C. Tanner, Z. Taylor, T. Mertzanidou, J. Cardoso, S. Ourselin, and D. J. Hawkes. Development of patient-specific biomechanical models for predicting large breast deformation. *Phys. Med. Biol.* 57:455–172, 2012.

[9]Holzapfel, G. A., T. C. Gasser, and M. Stadler. A structural model for the viscoelastic behavior of arterial walls: continuum formulation and finite element analysis. *Eur. J. Mech. A* 21:441–463, 2002.

[10]Hopp, T., M. Dietzel, P. A. Baltzer, P. Kreisel, W. A. Kaiser, H. Gemmeke, and N. V. Ruiter. Automatic multimodal 2D/3D breast image registration using biomechanical FEM models and intensity-based optimization. *Med. Image Anal.* 17:209–218, 2013.

[11]Kovacs, L., M. Eder, R. Hollweck, A. Zimmermann, M. Settles, A. Schneider, M. Endlich, A. Mueller, K. Schwenzer-Zimmerer, N. Papadopulos, and E. Biemer. Comparison between breast volume measurement using 3D surface imaging and classical techniques. *Breast* 16:137–145, 2007.

[12]Kovacs, L., M. Eder, R. Hollweck, A. Zimmermann, M. Settles, A. Schneider, K. Udosic, K. Schwenzer-Zimmerer, N. Papadopulos, and E. Biemer. New aspects of breast volume measurement using 3-dimensional surface imaging. *Ann. Plast. Surg.* 57:602–610, 2006.

[13]Kovacs, L., A. Yassouridis, A. Zimmermann, G. Brockmann, A. Woehnl, M. Blaschke, M. Eder, K. Schwenzer-Zimmerer, R. Rosenberg, N. Papadopulos, and E. Biemer. Optimization of 3-dimensional imaging of the breast region with 3-dimensional laser scanners. *Ann. Plast. Surg.* 56:229–236, 2006.

[14]Krouskop, T., T. Wheeler, K. Kallel, B. Garra, and T. Hall. Elastic moduli of breast and prostate tissues under compression. *Ultrason. Imaging* 20:260–274, 1998.

[15]Lapuebla-Ferri, A., A. D. Palomar, J. Herrero, and A.-J. Jimenez-Mocholi. A patient-specific FE-based methodology to simulate prosthesis insertion during an augmentation mammoplasty. *Med. Eng. Phys.* 33:1094–1102, 2011.

[16]Lee, A. W., V. Rajagopal, T. P. Babarenda Gamage, A. J. Doyle, P. M. Nielsen, and M. P. Nash. Breast lesion co-localisation between X-ray and MR images using finite element modelling. *Med. Image Anal.* 17:1256–1264, 2013.

[17]Mertzanidou, T., J. Hipwell, M. J. Cardoso, X. Zhang, C. Tanner, S. Ourselin, U. Bick, H. Huisman, N. Karssemeijer, and D. Hawkes. MRI to X-ray mammography registration using a volume-preserving affine transformation. *Med. Image Anal.* 16:966–975, 2012.

[18]Pathmanathan, P., D. Gavaghan, J. Whiteley, S. Chapman, and J. Brady. Predicting tumor location by modeling the deformation of the breast. *IEEE Trans. Biomed. Eng.* 55:2471–2480, 2008.

[19]Raith, S., M. Eder, F. von Waldenfels, J. Jalali, A. Volf, and L. Kovacs. Finite element simulation of the deformation of the female breast based on MRI data and 3-D surface scanning: an in vivo method to assess biomechanical material parameter sets. In: Proceedings of the 3rd International Conference and Exhibition on 3D Body Scanning Technologies, edited by N. D'Apuzo. Lugano: Hometrica Consulting, 2012, pp 196–203.

[20]Rajagopal, V., J. Chung, D. Bullivant, P. Nielsen, and M. Nash. Finite elasticity: determining the reference state from a loaded configuration. *Int. J. Numer. Methods Eng.* 72:1434–1451, 2007.

[21]Rajagopal, V., A. Lee, J. Chung, R. Warren, R. Highnam, and M. Nash. Creating individual-specific biomechanical models of the breast for medical image analysis. *Acad. Radiol.* 15:1425–1436, 2008.

[22]Rajagopal, V., P. M. F. Nielsen, and M. P. Nash. Modeling breast biomechanics for multi-modal image analysis—successes and challenges. *Wiley Interdiscip. Rev. Syst. Biol. Med.* 2:293–304, 2010.

[23]Roose, L., W. de Maerteleire, W. Mollemans, F. Maes, and P. Suetens. Simulation of soft-tissue deformations for breast augmentation planning. In: Lecture Notes in Computer Science: Biomedical Simulation, edited by M. Harders and G. Szekely. Berlin: Springer-Verlag, 2006, pp. 197–205.

[24]Samani, A., J. Bishop, M. Yaffe, and D. Pelwes. Biomechanical 3D finite element modeling of the human breast using MRI data. *IEEE Trans. Med. Imaging* 20:271–279, 2001.
[25]Samani, A., and D. Plewes. A method to measure the hyperelastic parameters of ex vivo breast tissue samples. *Phys. Med. Biol*. 49:4395–4405, 2004.
[26]Samani, A., J. Zubovits, and D. Plewes. Elastic moduli of normal and pathological human breast tissues: an inversion-technique-based investigation of 169 samples. *Phys. Med. Biol*. 52:1565–1576, 2007.
[27]Schnabel, J., C. Tanner, A. Castellano-Smith, A. Degenhard, M. Leach, R. Hose, D. Hill, and D. Hawkes. Validation of nonrigid image registration using finite-element methods: application to breast MR images. *IEEE Trans. Med. Imaging* 22:23–247, 2003.
[28]Sommer, G., M. Eder, L. Kovacs, H. Pathak, L. Bonitz, C. Mueller, P. Regitnig, and G. A. Holzapfel. Multiaxial mechanical properties and constitutive modeling of human adipose tissue: a basis for preoperative simulations in plastic and reconstructive surgery. *Acta Biomater*. 9:9036–9048, 2013.
[29]Tanner, C., J. H. Hipwell, and D. J. Hawkes. Statistical deformation models of breast compressions from biomechanical simulations. In: Lecture Notes in Computer Science: Digital Mammography, edited by E. A. Krupinsk. Berlin: Springer-Verlag, 2008, pp. 426–432.
[30]Tanner, C., J. Schnabel, D. Hill, and D. Hawkes. Factors influencing the accuracy of biomechanical breast models. *Med. Phys*. 33:1758–1769, 2006.
[31]van Houten, E., M. Doyley, F. Kennedy, J. Weaver, and K. Paulsen. Initial in vivo experience with steady-state subzone-based MR elastography of the human breast. *J. Magn. Reson. Imaging* 17:72–85, 2003.
[32]Wellman, P., R. Howe, E. Dalton, and K. Kern. Breast tissue stiffness in compression is correlated to histological diagnosis. Technical Report, Harvard Bio Robotics Laboratory, Division of Engineering and Applied Sciences, Harvard University, 1999, pp. 1–15.